

Electronic Supplementary Information

Assessment of Aggregative Growth of MnZn Ferrite Nanoparticles

Han-Wen Cheng^{a,b}, Jing Li^b, Season Wong[‡], and Chuan-Jian Zhong^{b*}

^a School of Chemical and Environmental Engineering, Shanghai Institute of Technology,
Shanghai 201418, China

^b Department of Chemistry, State University of New York at Binghamton, Binghamton,
NY13902, USA

Additional Experimental Data:

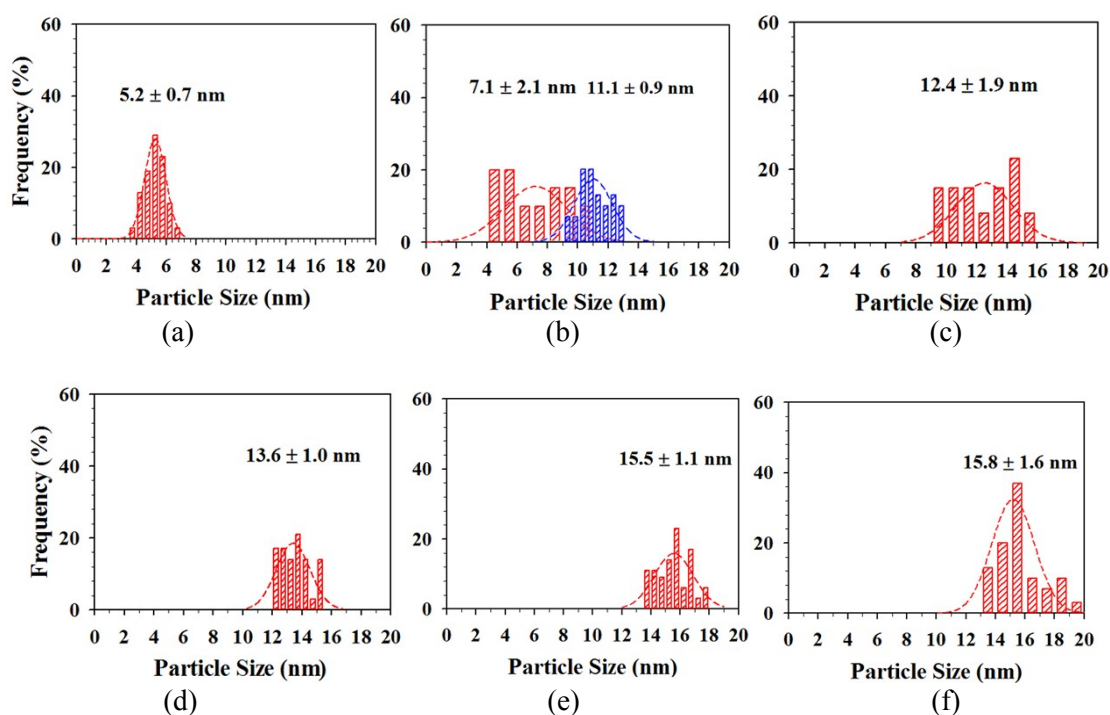


Fig. S1. Size distributions for MnZn ferrite nanoparticles synthesized at reflux temperature $T = 280\text{ }^{\circ}\text{C}$ (TEM images in **Fig. 1**) reaction time $t = 20$ (a, $5.2 \pm 0.7\text{ nm}$), 30 (b, $7.1 \pm 2.1\text{ nm}$; $11.1 \pm 0.9\text{ nm}$), 40 (c, $12.4 \pm 1.9\text{ nm}$), 50 (d, $13.6 \pm 1.0\text{ nm}$), 60 (e, $15.5 \pm 1.1\text{ nm}$) and 70 (f, $15.8 \pm 1.6\text{ nm}$) mins, respectively.

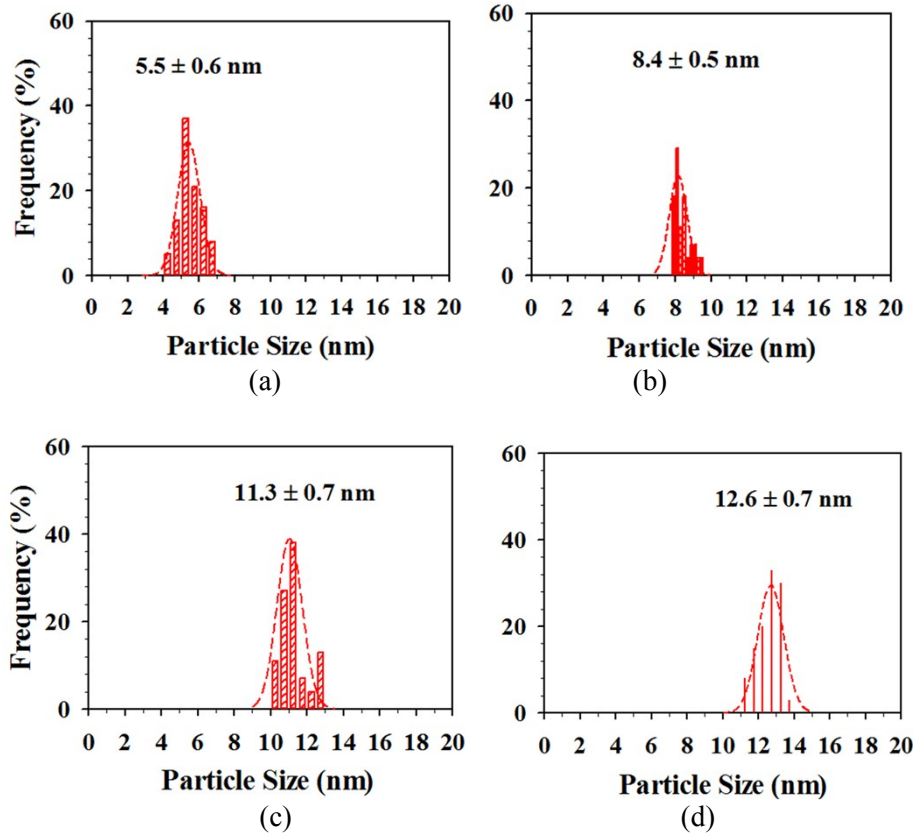
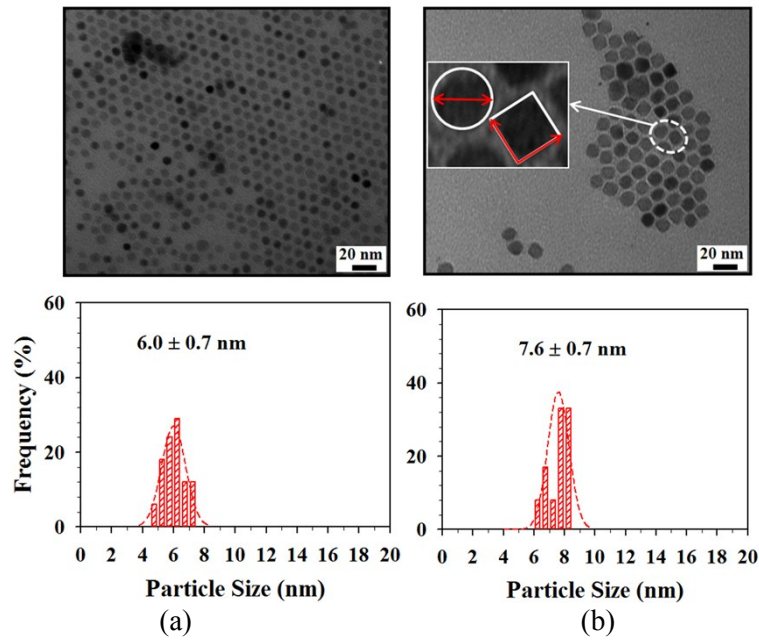


Fig. S2. Size distributions for MnZn ferrite nanoparticles synthesized at reflux temperature $T = 270$ °C (TEM images in **Fig. 3**), reaction time $t = 20$ (a, 5.5 ± 0.6 nm), 40 (b, 8.4 ± 0.5 nm), 60 (c, 11.3 ± 0.7 nm) and 80 (d, 12.6 ± 0.7 nm) mins, respectively.



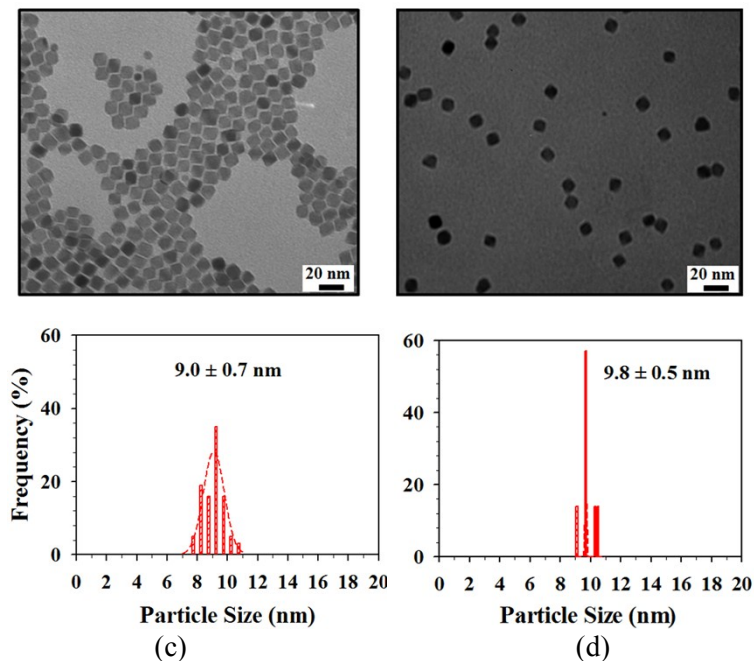


Fig. S3. TEM micrographs and size distributions for MnZn ferrite nanoparticles synthesized at reflux temperature $T=270\text{ }^{\circ}\text{C}$, reaction time $t=20$ (a, $6.0 \pm 0.7\text{ nm}$), 40 (b, $7.6 \pm 0.7\text{ nm}$), 60 (c, $9.0 \pm 0.7\text{ nm}$) and 80 (d, $9.8 \pm 0.5\text{ nm}$) mins, respectively. As indicated in (b), the overall average size of the particles was determined by measuring the diameters for the spherical particles and the side lengths for the cubic nanoparticles.

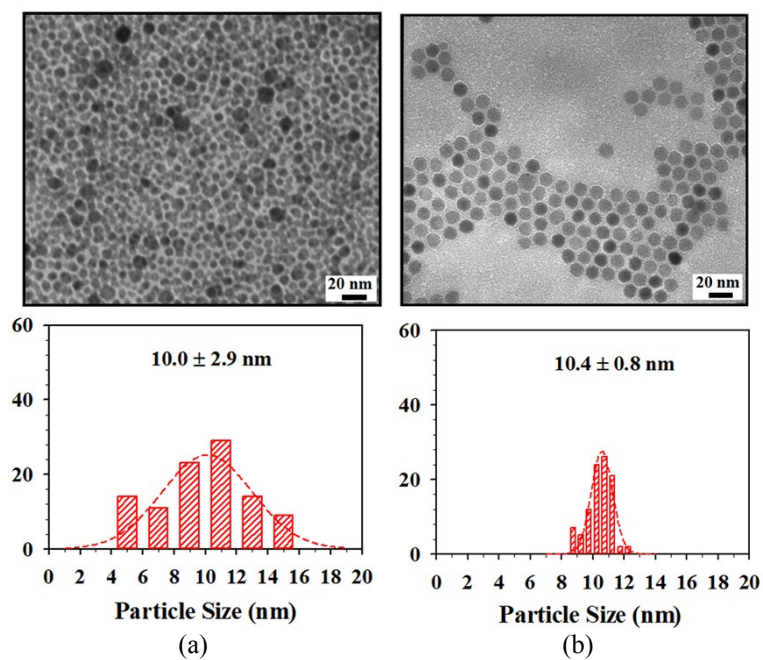


Fig. S4. TEM micrographs and size distributions for MnZn ferrite nanoparticles synthesized at reflux temperature $T=250\text{ }^{\circ}\text{C}$, reaction time $t=80$ mins (a, $10.0 \pm 2.9\text{ nm}$) and $T=260\text{ }^{\circ}\text{C}$, $t=80$ mins (b, $10.4 \pm 0.8\text{ nm}$).

Table S1. Composition and morphology of selected samples of MnZn ferrite nanoparticles analyzed by DCP-AES.

Temperature (°C)	Reaction time (min)	Composition	Shape & size (nm)
270	20	(Mn ²⁺ _{0.5} Zn ²⁺ _{0.5})Fe ³⁺ ₂ O ₄	Sphere (6.0 ± 0.7)
270	60	(Mn ²⁺ _{0.3} Zn ²⁺ _{0.7})Fe ³⁺ ₂ O ₄	Cube (9.0 ± 0.7)
240	60	(Mn ²⁺ _{0.3} Zn ²⁺ _{0.7})Fe ³⁺ ₂ O ₄	Cube (16.9 ± 1.8)
210	60	(Mn ²⁺ _{0.3} Zn ²⁺ _{0.7})Fe ³⁺ ₂ O ₄	Mostly sphere (9.9 ± 0.7)

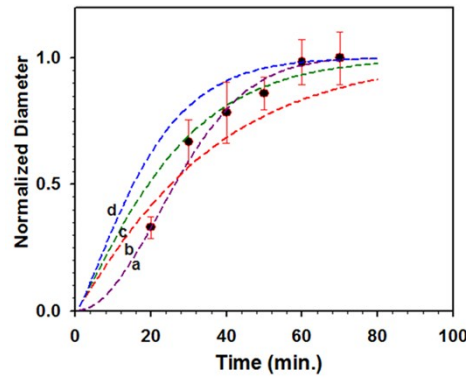


Fig. S5. A kinetic plot of the particle size for MnZn ferrite nanoparticles synthesized at reflux temperature $T = 280$ °C (data extracted from Fig. 1), reaction time $t = 20 \sim 70$ mins. Dashed lines: the theoretical fit based on Avrami model (eqn. (1)) yields (a) $k = 0.001 \text{ s}^{-1}$ and $n = 2$, (b) $k = 0.02 \text{ s}^{-1}$ and $n = 1.1$, (c) $k = 0.02 \text{ s}^{-1}$ and $n = 1.2$, (d) $k = 0.02 \text{ s}^{-1}$ and $n = 1.3$.

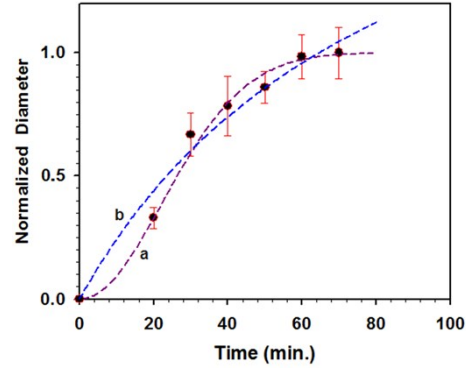


Fig. S6. A kinetic plot of the particle size for MnZn ferrite nanoparticles synthesized at reflux temperature $T = 280$ °C (data extracted from Fig. 1), reaction time $t = 20 \sim 70$ mins. Red dashed line (a): the theoretical fit based on Avrami model (eqn. (1)), yielding (a) $k = 0.001 \text{ s}^{-1}$ and $n = 2$. The experimental data are clearly

not fitted well by the “1+1” oriented attachment model [ref S1]: $D = \frac{D_0(\sqrt[3]{2} \times k_1 \times t + 1)}{k_1 \times t + 1}$, where D_0 and D

are the average size of primary particles and the average particle size at time t , respectively. k_1 is the rate constants for the model. Note that a general equation, $y = (1+a'x)/(b'+c'x)$, was used as simplified equation of the above equation in fitting the experimental data. In this case, the best fitting as shown by the blue

dashed curve (b) ($a' = 1.86 \times 10^6$, $b' = 6.8 \times 10^7$ and $c' = 8.0 \times 10^5$), which is apparently rather poor in comparison with the experimental data and Avrami model fitting (a).

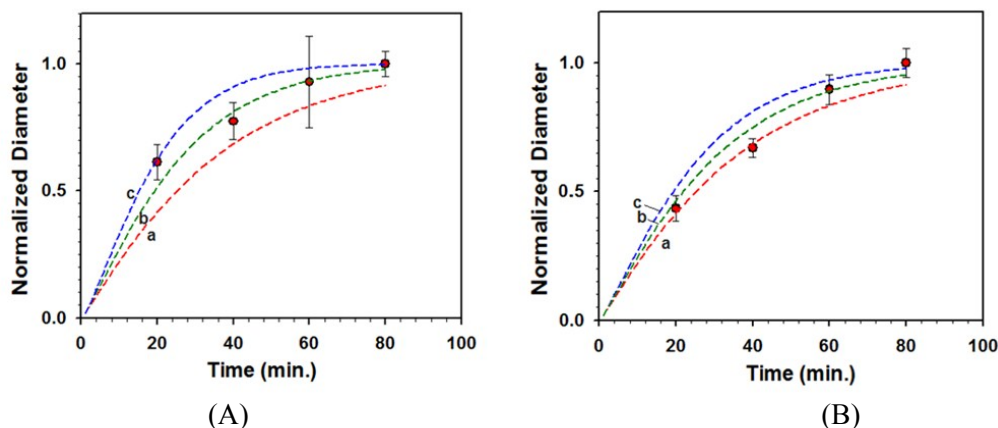


Fig. S7. Kinetic plots of the particle size for MnZn ferrite nanoparticles synthesized at reflux temperature $T = 270\text{ }^{\circ}\text{C}$, reaction time $t = 20 \sim 70$ mins, (A) data extracted from Fig. S3, (B) data extracted from Fig. 3. Dashed lines: the theoretical fit based on Avrami model (eqn. (1)) yields (A): (a) $k = 0.02\text{ s}^{-1}$ and $n = 1.1$, (b) $k = 0.02\text{ s}^{-1}$ and $n = 1.2$, (c) $k = 0.02\text{ s}^{-1}$ and $n = 1.3$, (B): (a) $k = 0.02\text{ s}^{-1}$ and $n = 1.1$, (b) $k = 0.02\text{ s}^{-1}$ and $n = 1.15$, (c) $k = 0.02\text{ s}^{-1}$ and $n = 1.2$.

Table S2. Summary kinetics analysis results:

Temperature ($^{\circ}\text{C}$)	Reaction time (min)	$k\text{ (s}^{-1}\text{)}$	n	Mean shape&size	Fig #
280 $^{\circ}\text{C}$	80	0.001	2	Cube ($\sim 15.9\text{ nm}$) ^a	Fig. 1 (f)
270 $^{\circ}\text{C}$	80	0.02	1.2 or 1.15	Cube (12.6 ± 0.7)	Fig. 3 (d)
260 $^{\circ}\text{C}$	80	0.02	1.4	Hexa (10.4 ± 0.8)	Fig. S4B
250 $^{\circ}\text{C}$	80			Sphere (10.0 ± 2.9)	Fig. S4A (b)

^a For a direct comparison of the size data, the 80-min particle size data were extracted from the curve fitting.

Reference:

[S1] X. G. Xue, R. L. Penn, E. R. Leite, F. Huang and Z. Lin, *CrystEngComm*, 2014, **16**, 1419-1429.